Lamination Frequencies as a Diagnostic for Horizontal Mixing in a 3D Transport Model*

CLARK J. WEAVER

Steve Myers and Associates, Vienna, Virginia

ANNE R. DOUGLASS AND RICHARD B. ROOD

NASA Goddard Space Flight Center, Greenbelt, Maryland

(Manuscript received 24 June 1998, in final form 10 March 1999)

ABSTRACT

Ozone simulations are performed in an attempt to simulate laminar events with the frequency observed in balloon ozone sondes. The winds are taken from the Goddard Earth Observing System Data Assimilation System (GEOS DAS); the importance of horizontal and vertical resolution to production of lamina are investigated. A simulation with a high horizontal reolution (grid spacing 1° latitude by 1.25° longitude) and high vertical resolution (~300 m grid spacing) isentropic model produces lamination frequencies close to the balloon sonde climatology near the polar vortex edge but exhibits too much lamination in the subtropics. This indicates that the GEOS DAS winds contain the information to produce laminar events, although such small-scale features are not manifest in the more commonly used 2° latitude by 2.5° longitude transport model, which uses the hybrid sigma-pressure vertical coordinate. The zonal average ozone tendencies due to horizontal mixing in the lamina-producing models are similar to the tendencies in coarser resolution models that show no lamination, suggesting that it is not necessary to resolve laminar events to maintain a realistic ozone budget. The comparison of the modeled lamination frequency with the balloon sonde climatology indicates that the model horizontal mixing at the vortex edge is accurate but in the subtropics the mixing is excessive.

1. Introduction

In an averaged sense, tracer distributions in the stratosphere are determined by a balance between ''slow'' transport by the residual circulation and the accumulated impact of quasi-isentropic ''fast'' transport by Rossby waves (Mahlman 1985). Achieving the correct representation of this balance has been a challenge for three-dimensional transport models simulating stratospheric constituents. Long integrations of the Goddard off-line chemistry and transport model (CTM) using early versions of the National Aeronautics and Space Administration (NASA)/Goddard Data Assimilation System were not realistic because the residual circulation was too strong (Weaver et al. 1993). Constituent simulations of ozone and nitric acid showed that observed synoptic-scale features were captured by the model; however, after a few months of integration, unrealistic biases overwhelmed the results (Rood et al. 1991; Allen et al. 1991). The residual circulation is dramatically improved in a more recent version of the Goddard Earth Observing System Data Assimilation System (GEOS DAS) described by Schubert et al. (1993). Douglass et al. (1996) successfully used these winds for a year-long ozone simulation. Even after a year, the lower stratospheric horizontal and vertical gradients are realistic and the model captures synoptic-scale events observed by the *Nimbus-7* Total Ozone Mapping Spectrometer (TOMS). Comparison of the year-long ozone simulation with satellite data showed that in the lower stratosphere and upper troposphere the model has a slight buildup of ozone in the midlatitudes and a deficit in the Tropics. This excessive latitudinal gradient of lower stratospheric ozone can be interpreted as an improper balance between the residual circulation and the horizontal mixing in the model. A simple comparison of modeled and observed latitudinal gradients does not reveal the extent to which these two competing processes are modeled poorly.

This paper assesses the model horizontal mixing by comparing frequency of lamination generated by the model with the frequency of lamination observed in the

* NASA/GSFC Stratospheric General Circulation with Chemistry Project Contribution Number 84.

Corresponding author address: Dr. Clark Weaver, NASA/GSFC, Code 916, Greenbelt, MD 20771.
E-mail: weaver@demeter.gsfc.nasa.gov

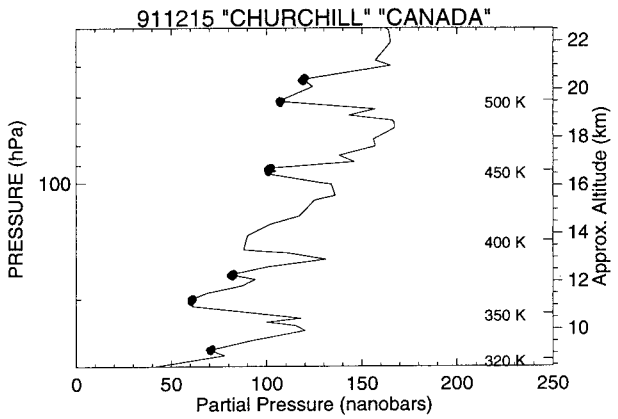

FIG. 1. Single ozone profile from a balloon sonde at Churchill, Canada, 1500 UTC 14 Dec 1991. The dots are minimum values associated with each lamina feature.

ozone sonde profiles. This is related to horizontal mixing, at least in the vicinity of strong latitudinal gradients of ozone. This often occurs at the edge of the polar vortex as wave breaking events cause filamentation at the interface. The filaments are actually sheets that elongate and thin as they are peeled off the interface edge. Since the filamentation process is irreversible, it is a likely precursor to horizontal mixing. Vertical shear in the horizontal wind will tilt and distort the filament sheets and cause local ozone minima or maxima in an ozone profile. This vertical shear is induced by either planetary, synoptic, or gravity waves.

Many laminar features are seen in an observed ozone profile (Fig. 1) from Churchill, Canada (58.8°N, 265.9°E). Minimum values associated with each lamina feature are marked. The criteria for lamination in this study is the same used by Reid and Vaughn (1991) and is described in section 4. Of course we cannot expect the model to capture structure smaller than the vertical resolution of the model (about 1 km in the upper troposphere). Of interest is the level of detail of these finescale features that must be modeled to capture the accumulated impact of the quasi-isentropic mixing. Although the ozone simulation is not perfect, the transport model maintains realistic latitudinal and vertical gradients, indicating that the transport model does a reasonable job of simulating the net mixing; that is, the model must capture the net effect of horizontal mixing even though horizontal resolution is too coarse to simulate actual mixing processes. This hints that we should not be concerned that the standard transport model rarely simulates ozone lamina. Our interest is to reconcile the model's reasonable mean horizontal and vertical constituent gradients with the lack of lamina structure in the model profiles. We are motivated to see if the assimilated winds contain sufficient wind shear to produce the observed vertical structure for simulations run at high horizontal and vertical resolution. If we can construct a model with sufficient resolution to simulate lamina, then we can compare the model lamination frequencies with an observed climatology. This requires that the model produce the statistics of the laminar structure. Some of the simulated laminae may be actual observed features but others may not. Budget calculations for the standard resolution and the higher resolution models should reveal whether the increased resolution and the presence of lamination significantly alters the net horizontal mixing in the transport model.

Comparison of the modeled lamination frequencies with the observed climatology should reveal if the horizontal mixing is realistic. This information should clarify whether insufficient horizontal mixing or an excessively strong residual circulation causes the steeper than observed latitudinal gradients in the modeled ozone.

Section 2 describes the various transport models used in this study. Since the integrations are short term, the initialization method is important and is discussed in section 3. Section 4 presents model comparisons with satellite and ozone sonde data, a comparison of lamination frequencies in the model compared with climatology derived from balloon sonde profiles, and ozone budgets from the various models. A discussion and summary follow.

2. Transport models

We employ two off-line three-dimensional chemistry and transport models (CTMs) that have different vertical grids. One model uses a hybrid sigma-pressure coordinate and the other is formulated in isentropic coordinates. Both are driven by off-line winds from the GEOS DAS assimilation system that are archived every 6 h on 46 vertical sigma levels at 2° latitude by 2.5° longitude horizontal resolution. The winds used here are from a version of GEOS DAS that has several improvements over the version used by Douglass et al. (1996). A major change is the placement of the computational pole in the assimilation general circulation model at the equator (Takacs and Suarez 1995). This significantly reduces the noise in the polar regions. Changes to the tropical field of Ertel's potential vorticity (EPV) are minimal because the Coriolis parameter tends to zero. Both CTMs include parameterized chemical production and loss taken from the Goddard 2D model (Douglass et al. 1989; Jackman et al. 1996). Advection is accomplished using a three-dimensional flux form semi-Lagrangian scheme (Lin and Rood 1996). To study the ozone transport budget, the tendencies due to horizontal and vertical advection are archived.

a. Sigma-pressure transport model

This study uses a hybrid sigma-pressure coordinate with two different vertical grid resolutions. One is the standard Goddard three-dimensional transport model, which was designed to transport many constituents for long-term integrations in tandem with a full chemistry

module. It has 29 vertical levels, 11 sigma levels between the surface and an interface at 130 hPa, and 18 pressure levels between the interface and 0.4 hPa. In the lower stratosphere the vertical grid spacing is about 1 km. The standard 29-level transport model uses a monotonic piecewise parabolic method (PPM) transport scheme in the horizontal. A less diffusive positive-definite PPM is used in the vertical direction. In the standard model the vertical transport is decoupled from the horizontal transport and computed independently. The result is that cross-derivative terms associated with the vertical and horizontal advection are ignored.

We have designed a second hybrid sigma-pressure coordinate model with higher vertical resolution in an effort to simulate features of lamination. This CTM has 73 vertical levels and a vertical grid spacing of about 200 m in the lower stratosphere. In contrast to the standard model, the advection scheme does account for the cross-derivative terms associated with the vertical and horizontal advection by using a modified multidimensional flux correction (MFC) option (Zalesak 1979). The transport scheme that used MFC employs unconstrained PPM in all directions and is nearly diffusion free.

The GEOS DAS winds are output on 46 levels and must be placed on the model grid. Where the vertical resolution of the transport grid is less than the resolution of the original winds (i.e., where the 73-level model has vertical grid spacing of 200 m), this is accomplished by linear interpolation. Where the transport grid resolution is coarser than the original winds, simple linear interpolation introduces unwanted noise in the vertical velocity fields. In these regions, the winds from GEOS DAS assimilation system are mapped onto the transport grid using a scheme that minimizes the interpolation noise (S. J. Lin 1997, personal communication). This scheme is used to map winds onto the 29-level vertical grid and in the 73-level model where the vertical resolution is coarse.

b. Isentropic transport model

Three-dimensional isentropic transport models have been used elsewhere to simulate weather events in the troposphere and chemical processes in the Arctic polar stratosphere. For example, Zapotocny et al. (1993) use a hybrid isentropic-sigma transport model to simulate the northward advection of water vapor and subsequent precipitation during the January 1979 Chicago blizzard. Chipperfield et al. (1997) use an isentropic transport model to simulate chlorine deactivation and the formation of the chlorine nitrate collar in the Arctic vortex. This application of an isentropic model to simulation lamination follows the work of Orsolini (1995). In this work, lamina events were simulated using a series of vertically stacked, horizontal isentropic models.

The three-dimensional isentropic transport model used in our study has 46 vertical levels that range from 320 to 2000 K. In the vertical region where lamination is expected (320–500 K) the grid has a 5-K resolution (at 60°N this is approximately 300-m resolution); elsewhere it is coarser. At the model boundaries, 320 and 2000 K, the vertical velocity is nonzero and the ozone mixing ratios are held fixed at their initial values. This allows ozone mass to flow through the top and bottom boundaries.

There are different ways to implement the isentropic model. The horizontal winds are interpolated to isentropic surfaces, and the vertical velocity is calculated from the isentropic continuity equation using the horizontal winds and temporal pressure tendencies on isentropic surfaces. Constituent distributions calculated using this CTM are similar to those from the sigma-pressure transport model. Vertical velocities from continuity tend to be noisy due to unrealistic gravity waves in the general circulation model (GCM) used in the assimilation procedure and also due to the wind and temperature increments that force the assimilation GCM toward the observations. The use of the wind-mapping scheme reduces these effects but the calculated vertical winds are still noisy. This noise is dependent on the wind dataset used and is not inherent it the sigma-pressure formulation.

The vertical velocities can also be calculated from diabatic heating rates. The heating rates used in this study are the sum of the shortwave, longwave, turbulent, and moist heating from GEOS DAS. Of these, the radiative terms are the largest contributors to the total heating rate. The assimilation temperature increments that force the assimilation GCM toward the observations are not included in the diabatic heating rates. These vertical velocities are generally at least an order of magnitude smaller than those derived from continuity, since continuity-derived vertical velocities include the diabatic component of the velocity and the much larger adiabatic component. Those from heating rates include only the smaller diabatic component.

The horizontal winds that have been mapped onto the isentropic surfaces can drive the transport model when the diabatic heating rates are used as the vertical velocities; however, a mass correction term must be added because the divergence of the winds is not consistent with the diabatic heating rates. For GEOS DAS winds, the mass correction term can be the same order as the vertical advection term and thus render any ozone budget calculation questionable. The SLIMCAT isentropic model (Chipperfield 1999) requires a mass correction term because the horizontal winds are not in balance with the vertical velocities. Here we minimize the mass correction term by adjusting the horizontal winds so that the divergence agrees with the heating rates while preserving the original vorticity. This is accomplished by the following procedure. The vorticity of the original winds is calculated on isentropic levels. At each layer the mass divergence is calculated from the isentropic thermodynamic equation, using the assimilation diabatic heating rate and temperature tendency. A set of ‘‘ad-

TABLE 1. Description of transport models.

Vertical coordinate	Vertical levels	Vertical velocity	Horizontal grid spacing	Time step (s)	Label
Sigma-p	29	Continuity	2° × 2.5°	900	SP-C-29
Sigma-p	73	Continuity	2° × 2.5°	900	SP-C-73
Isentropic	46	Diabatic heating rates	2° × 2.5°	900	IS-H-46
Isentropic	46	Diabatic heating rates	1° × 1.25°	450	IS-H-46-HR
Isentropic	46	Continuity without adiabatic part	2° × 2.5°	900	IS-C-46

justed'' winds is derived from this new divergence and the original vorticity. The adjustment alters the divergence of the winds but not the vorticity. Changes to the horizontal wind velocity are less than 0.1 m s^{-1}, but the changes to the vertical velocity are significant. This is similar to the procedure used by Weaver et al. (1993) to make the residual circulation calculated from the definition equivalent to the residual circulation calculated from the diabatic heating. In this study, this procedure to adjust the winds is only used in this application of the isentropic model, that is, when the diabatic heating rates are used as the vertical velocities.

3. Ozone-mapped EPV fields

An initial condition for the ozone integrations can be derived from EVP fields for a given day using a relationship between ozone from balloon sondes and EPV. This approach is similar to the constituent reconstruction method described in Schoeberl et al. (1989), Douglass et al. (1989), and Lary et al. (1995). It capitalizes on the good correlation between ozone and EPV on isentropic surfaces near the tropopause (Riishojgaard and Kallen 1997). The sondes are the only source of ozone data in the altitude region where lamination is generally observed. An EPV–ozone relationship is derived on each model isentropic level using 10 years of balloon ozone sondes from the World Meteorological Organization World Ozone Data Center and EPV fields from the National Centers for Environmental Prediction (NCEP). For each model isentropic level the initial ozone field is derived using this relationship and the EPV field of the initial winds.

The initialization is in near balance with the driving wind fields and minimizes transient transport that occurs as the ozone field adjusts to the transport model. A comparison of the data from the microwave limb sounder (MLS) at the 44-mb retrieval level with the mapped ozone field interpolated to that level shows that the mapped field captures the observed synoptic-scale features, although it does not attain the maximum and minimum values seen in the MLS data.

4. Results

With this initialization we ran versions of the sigma-pressure model and the isentropic model from 6 to 23 December 1991. Table 1 lists all model configurations used in this study. The abbreviations used in the labels are isentropic (IS), sigma-pressure (SP), heating rates (H), continuity (C), and high horizontal resolution (HR). Except for the 1° × 1.25° run, all simulations had the same horizontal grid spacing as the assimilated winds, 2° latitude by 2.5° longitude. Before the model results are analyzed for lamination frequencies and budget terms, we evaluate the accuracy of the simulations with satellite observations.

a. TOMS and ozone sondes

Figures 2 and 3 show latitude versus longitude and zonal mean comparisons of the TOMS data with the standard sigma-pressure model SP-C-29, the high vertical resolution sigma-pressure model SP-C-73, and the isentropic model IS-H-46 at the end of the integration. In the analysis we focus on the changes in the total column ozone during the integration because the total column initialization is offset from the TOMS observations. Altering the initialization to match TOMS introduces unrealistic lamination at the beginning of the integration. The offset is less than 15 Dobson units (DU) in the Northern Hemisphere.

After 26 days of integration both models capture the location and magnitude of the midlatitude synoptic-scale features in the TOMS data. In the Tropics the isentropic model represents the zonal symmetry of the TOMS data.

Neither of the models simulates the TOMS latitudinal ozone distribution. During the integration the tropical midlatitude gradient of TOMS steepens as ozone builds in the midlatitudes and the latitude of maximum column ozone shifts equatorward. The sigma-pressure models capture this shift in latitude of maximum column ozone but have too much midlatitude buildup and a slight deficit in the Tropics. These biases in the sigma-pressure

→

FIG. 2. Total column ozone on 31 Dec 1991 from (a) TOMS, (b) the 29-level sigma-pressure model SP-C-29, (c) the 73-level model SP-C-73, and (d) the isentropic model IS-H-46. Model runs are at 2° latitude by 2.5° longitude horizontal resolution and are after 25 days of integration. The contour interval is 19 DU.

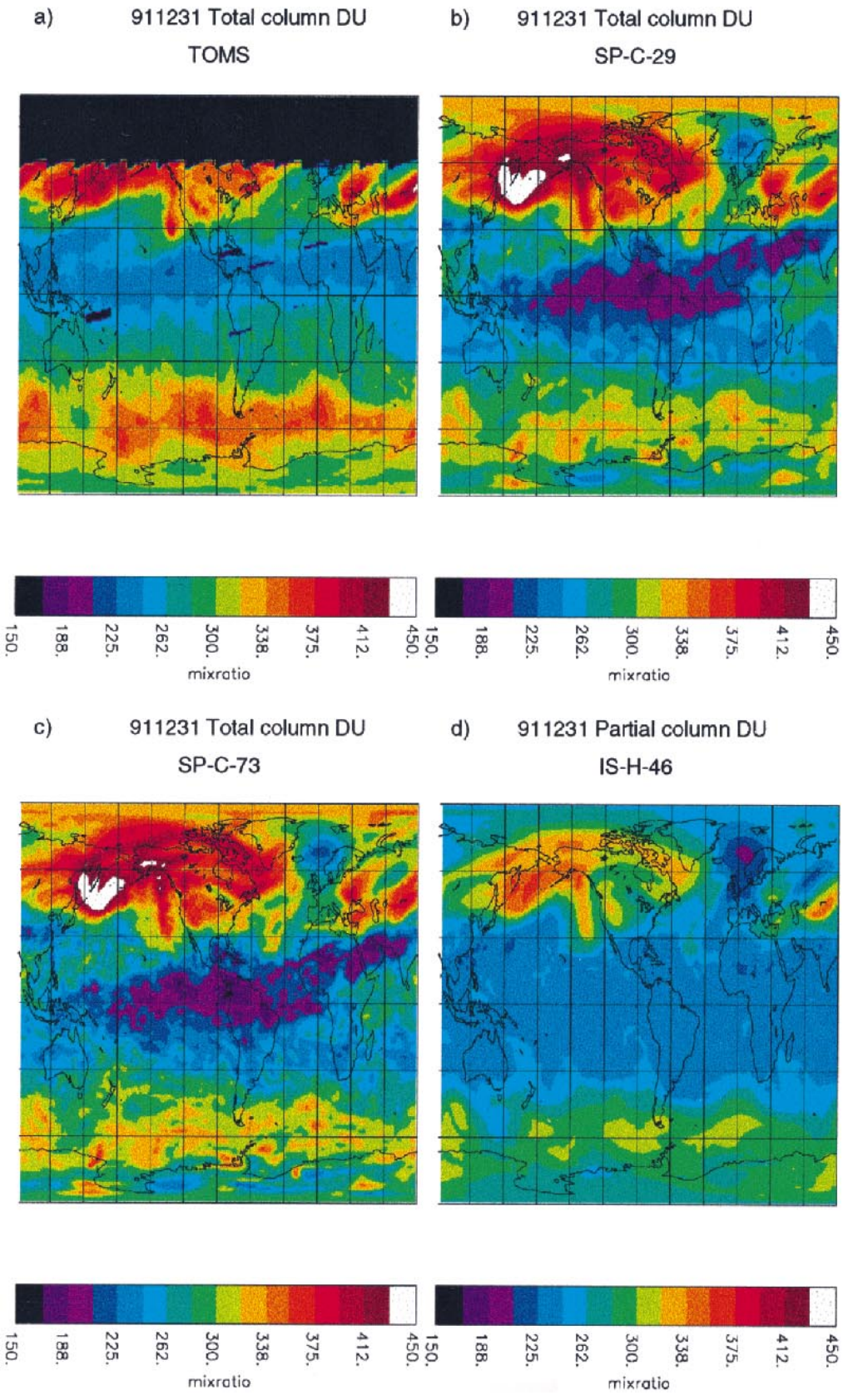
a)
911231 Total column DU
TOMS
b)
911231 Total column DU
SP-C-29
150.
188.
225.
262.
300.
338.
375.
412.
450.
mixratio
c)
911231 Total column DU
SP-C-73
d)
911231 Partial column DU
IS-H-46

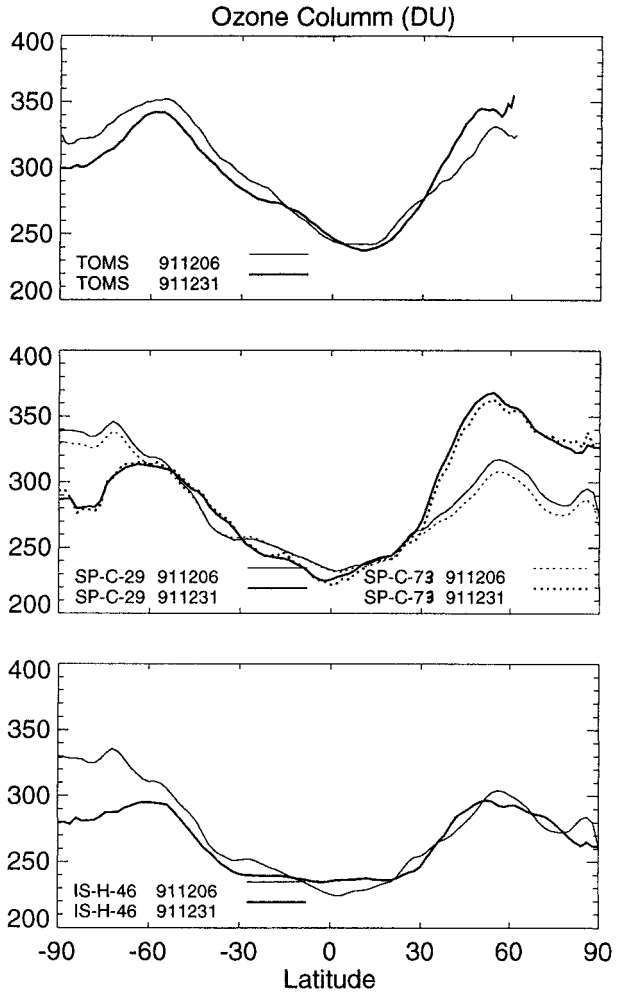

FIG. 3. Zonal mean total column ozone for the initialization on 6 Dec 1991 and 25 days later on 31 Dec 1991 for (a) TOMS, (b) two sigma-pressure models, and (c) the isentropic model IS-H-46. Model runs are at 2° latitude by 2.5° longitude horizontal resolution.

model are consistent with biases reported by Douglass et al. (1996).

The results from the isentropic model are very different. Since the model does not extend to the earth's surface, only a partial column of ozone above the 320-K isentropic surface is shown. Based on the initialization, the missing ozone below 320 K is about 15 DU in the northern midlatitudes and less in the Tropics. It is clear from Fig. 3c that the midlatitudes show no sign of buildup during the integration. In the Tropics the values increase from the initial 220 DU near the equator. The zonal mean total column ozone initially increases close to the equator; as the integration proceeds, points farther from the equator also increase. At the end of the integration the entire region 30°S–30°N has attained a constant 240-DU value.

We also compared the model vertical profiles with balloon sondes. Figure 4 shows profiles from the only two tropical stations, and a selection of extratropical stations. The Ascension Island and Brazzaville sondes on 6 Dec 1991 verify initialization in the Tropics. During the integration the isentropic model hugs the sonde but the sigma-pressure model (SP-C-29) has a systematic negative bias consistent with the tropical TOMS bias. Both models accurately reproduce observed profiles at the subtropical station in Naha, Japan, but the isentropic model shows vertical structure not seen in the sondes. This is most pronounced on 9 and 11 December 1991 between 400 and 500 K. Smaller-scale structure is also apparent later in the integration 17 and 18 December 1991 between 400 and 450 K. The only other subtropical station, in Irene, South Africa (not shown), also shows more vertical structure in the model compared to the sondes. At the midlatitude Hohenpeissenberg station the sigma-pressure model has high values compared with the soundings—again consistent with the high bias compared with the TOMS data. In the lower stratosphere the isentropic model sometimes hugs the soundings but on other days is low. Sondes from the higher-latitude stations show more vertical structure than those closer to the equator. Although neither model reproduces specific lamina events, the isentropic model shows more vertical structure.

The model results shown in Figs. 2, 3, and 4 used a 2° latitude by 2.5° longitude resolution. The isentropic model also was run at a higher 1° latitude by 1.25° longitude resolution (IS-H-46-HR). Total column ozone plots and vertical profiles from the high-resolution run are almost identical to those shown here. However, the lamination frequencies are different.

b. Lamination frequencies

Reid and Vaughn (1991) present a survey of the scale and spatial distribution of ozone lamination using balloon sondes launched from 20 stations mostly in the Northern Hemisphere. We adopt their definition so that their climatology of ozone lamination frequencies provides context for our results. The vertical extent of the lamina must be between 200 m and 2.5 km; the excursion from the large-scale profile must be greater than 20 nb of ozone partial pressure. Since the highest vertical resolution of the models used in this study has a grid spacing of about 200 m, we do not expect to simulate laminae of the finest scale. This should not be a problem since the mean laminar width derived from observations is 1–1.5 km (Reid and Vaughan 1991), easily resolved by a 200-m resolution grid.

Figure 5 shows a comparison of lamina probabilities from the sonde climatology and from a model. Both figures show the probability of lamination, $P_l(\Delta\phi, z)$, at a given latitudinal distance from the vortex edge ($\Delta\phi$) and altitude (z). The latitudinal distance from the vortex edge was calculated using NCEP winds. Details on the calculation of the vortex edge are given in Nash et al. (1996).

The probability of lamination is calculated from P_l

$= P_{sl}/P_s$, where P_{sl} is the probability that a profile (from the population of sondes or model profiles) will include a lamina event and P_s is the probability that the population of profiles will sample a $(\Delta\phi)$ and altitude. Here P_s accounts for the fact that there are more stations at higher latitudes than lower but the model has the same number of vertical profiles at each latitude.

Figure 5a shows lamina frequencies from a December–January climatology of the balloon sondes. Frequencies below 13 km are not shown. The lamination frequency decreases with latitude equatorward of the vortex edge. The lamination is most likely to occur at a lower altitude poleward of the vortex edge, but there is no systematic latitudinal decrease.

Figure 5b shows lamina frequencies from the 1° latitude by 1.25° longitude isentropic model IS-H-46-HR. In the stratosphere there is a local maximum slightly equatorward of the vortex edge; frequencies decline with latitude away from the edge. A second maximum exists between 30° and 60° equatorward of the polar vortex. A figure similar to Fig. 5b plotted as a function of latitude rather than the distance from the vortex edge places this maximum between the equator and 30°. Using balloon sonde data, Reid et al. (1993) present a similar figure in terms of potential temperature and latitude (their Fig. 1a). The location of their maximum is 400 K (13–15 km) and is consistent with Fig. 5a. It is difficult to compare the magnitude of the maximum because they do not account for the spatial variability of the vortex edge.

Figure 6 shows vertically integrated lamination rates in the stratosphere for three different models compared with the balloon sondes. The isentropic model with the 1° latitude by 1.25° longitude resolution, IS-H-46-HR, shows the highest lamination probabilities. This model has too much lamination in the subtropics but not enough near the polar vortex. The excess subtropical lamination in the model is consistent with the finescale structures seen in the model profiles near the subtropical stations of Naha, Japan, and Irene, South Africa, but not seen in the actual soundings (Fig. 4). Degrading the horizontal resolution to a grid spacing of 2° latitude by 2.5° longitude (IS-H-46) reduces the lamination probabilities. The sigma-pressure model SP-C-73 shows the least lamination but retains the bimodal distribution with peaks in the subtropics and near the polar vortex.

c. Budgets

Calculating the individual terms of the ozone continuity equation lends insight toward understanding the differences between the various models used in this study. The transport model solves the constituent continuity equation in the flux form, but it is not possible to separate the effect of the residual circulation and horizontal mixing with this formulation. Instead, we show terms from the transformed Eulerian mean (TEM) formulation, which separates mixing and advective processes [Andrews et al. 1987, Eq. (9.4.13)]:

$$\overline{\rho}\,\overline{\chi}_t + \overline{\rho}\,\overline{v}^*\overline{\chi}_y + \overline{\rho}\,\overline{\omega}^*\overline{\chi}_p - \nabla\cdot\mathbf{M} - \overline{\rho}\overline{S} = \text{balance},$$

where the overbar denotes the zonal mean, χ is the ozone mixing ratio, S is the chemical source, * signifies a residual velocity, and ρ signifies the density. Subscripts represent differentials. The $\nabla\cdot\mathbf{M}$ represents the effects of horizontal mixing. Figure 7 shows the zonal mean terms from the TEM constituent continuity equation from the SP-C-29 and SP-C-73 model integrations in the region of the atmosphere where lamination occurs. The residual circulation terms are $\overline{\rho v}^*\overline{\chi}_y + \overline{\rho\omega}^*\overline{\chi}_p$. These terms transport low-ozone air upward in the Tropics and ozone-rich air downward at middle and high latitudes (poleward of 30°N). This transport is balanced by horizontal mixing and local time change terms. The balance term is nonzero due to imprecise numerics. The budgets presented in Fig. 7 are not sensitive to the vertical grid spacing, which is about 1 km in the standard model (SP-C-29) and about 200 m in the high vertical resolution model (SP-C-73).

Comparison of the budgets from the sigma-pressure models with the isentropic model must account for the fact that surfaces of constant sigma and pressure are not parallel with surfaces of constant potential temperature. Projecting components of the sigma-pressure fluxes onto isentropic surfaces will introduce errors. Instead, the isentropic model was rerun using the GOES DAS winds mapped onto the 46 isentropic levels, using the same procedure as is used to map the winds to a higher-resolution grid in the sigma pressure model, and omitting the adjustment procedure used in IS-H-46. The vertical winds are calculated from continuity. In the region of interest, where there is a high density of isentropic surfaces, results from IS-C-46 are very similar to the standard sigma-pressure run SP-C-29. The vertical movement of parcels with respect to altitude are almost identical in both models because the diabatic and the adiabatic component of the vertical velocities are the same. In IS-C-46 the adiabatic component of the vertical velocity translates the isentropic vertical coordinate system with respect to altitude. In SP-C-29, the adiabatic component is part of the vertical velocity. This suggests that with sufficient resolution results are not dependent on model formulation. The results from IS-H-46 look very different than the continuity runs. The movement of the isentropic surfaces with respect to altitude is the same as in IS-C-46, so the adiabatic components are the same for all three models. However, the diabatic component of the vertical velocity is different for IS-H-46 because it is derived from the assimilation heating rates. It would be possible to modify the winds in the sigma-pressure model so that the diabatic component would be consistent with the assimilation heating rates. Although we have not done this run, the results should be very similar to IS-H-46.

Figure 8 shows ozone mass budget terms within the

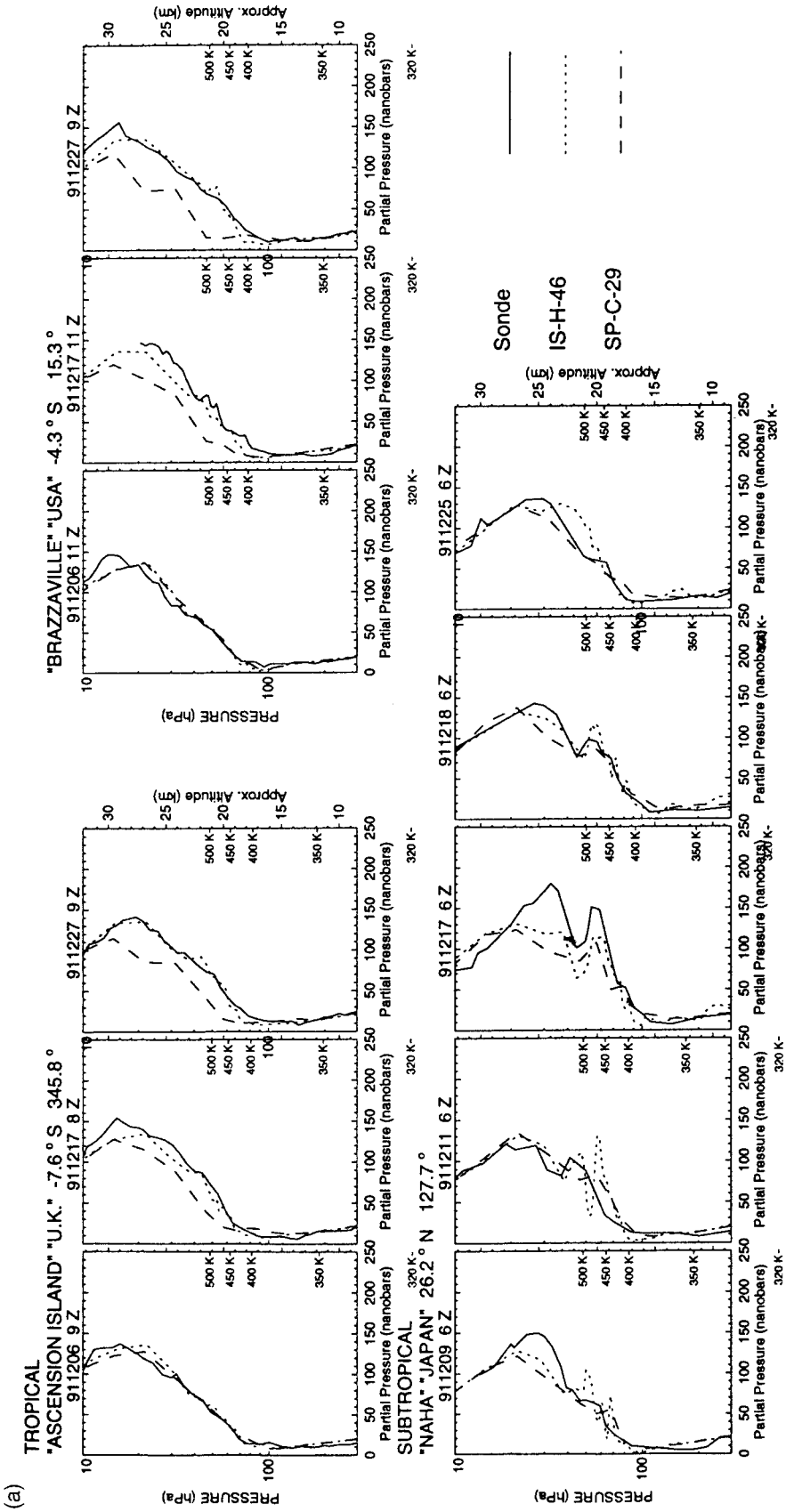

FIG. 4. Vertical profiles of ozone from balloon sonde observations, the isentropic model IS-H-46, and the sigma-pressure model SP-C-29 for (a) Ascension Island, 8°S, 345°E; (b) Brazzaville, 4°S, 15°E; (c) Naha, Japan, 26°N, 128°E; (d) Hohenpeissenberg, 48°N, 11°E; (e) Goose Bay, Canada, 53°N, 300°E; (f) Churchill, Canada, 58°N, 265°E; (g) Resolute, Canada, 75°N, 265°E; and (h) Alert 83°N, 298°E. A potential temperature scale is shown on the right.

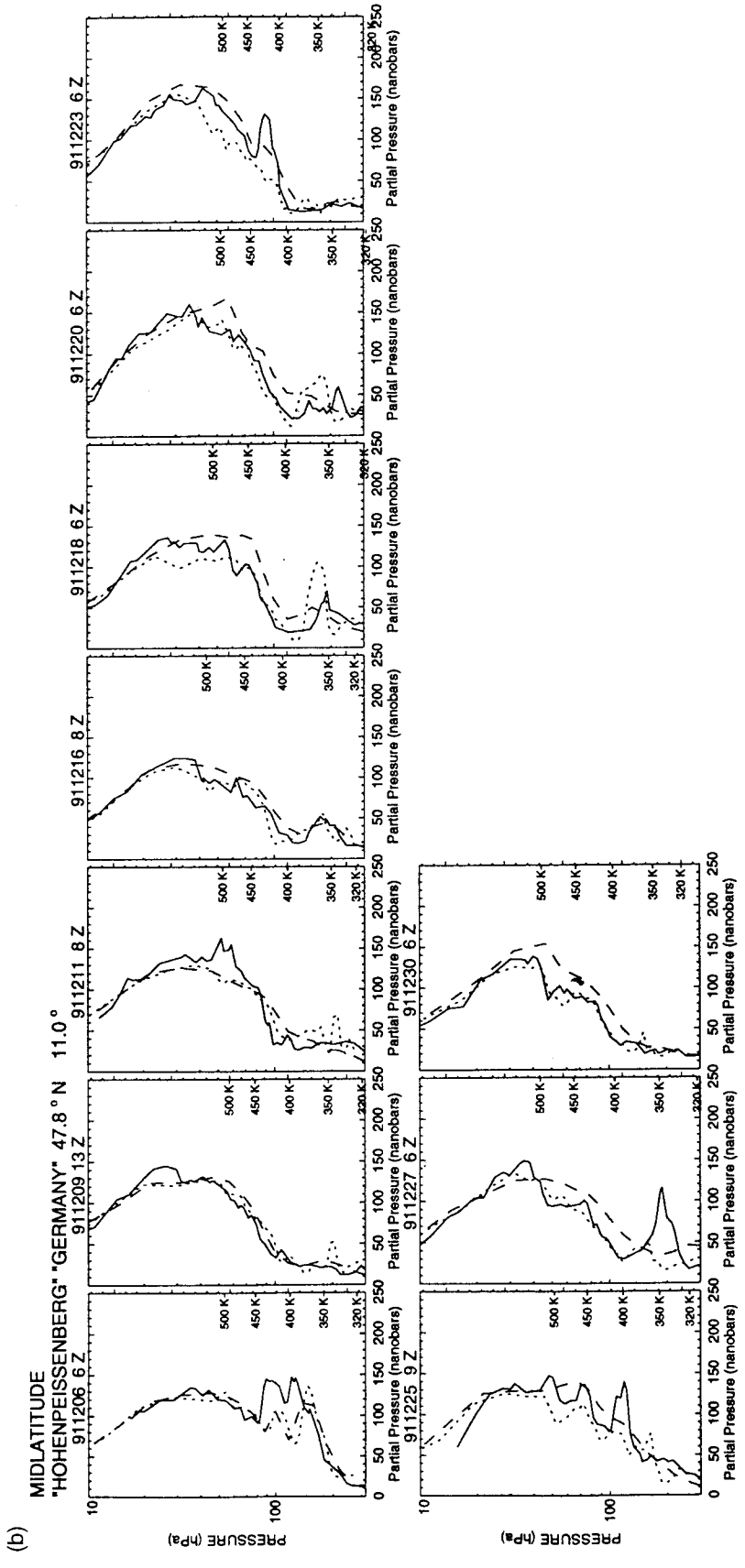

FIG. 4. (*Continued*)

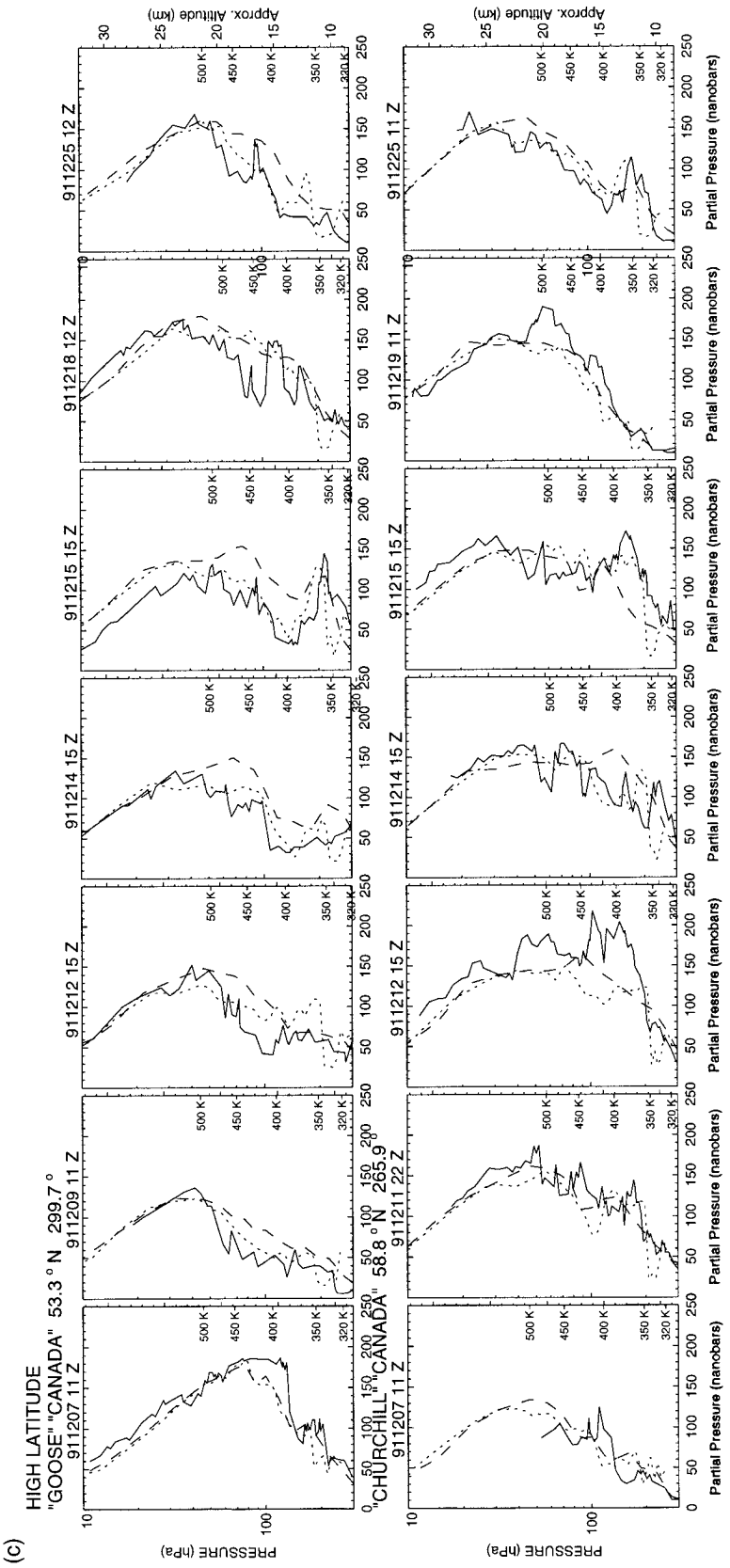

FIG. 4. (*Continued*)

potential temperature surfaces where lamination occurs from the IS-H-46 and IS-C-46 integrations. Recall that the vertical velocities for IS-H-46 are taken directly from the assimilation diabatic heating rates. Since IS-C-46 is also an isentropic coordinate model, the continuity-derived vertical velocities do not include the adiabatic component. These budget terms are from the advective form of the ozone continuity equation [Andrews et al. 1987, Eq. (9.4.19)]:

$$\overline{\sigma}\,\overline{\chi}_t + (\overline{\sigma'\chi'})_t + (\overline{\sigma v})\overline{\chi}_y + [\overline{(\sigma v)'\chi'}]_y + (\overline{\sigma Q})\overline{\chi}_\theta + [\overline{(\sigma Q')\chi'}]_\theta = \overline{\sigma S},$$

where σ is the density in isentropic coordinates $-g^{-1}p_\theta$, Q is the diabatic heating rate, θ is the potential temperature, and primes are the perturbation from the zonal mean. In the horizontal direction the eddy term $[\overline{(\sigma v)'\chi'}]_y$ is a result of isentropic mixing, which tends to break down the ozone gradient between the Tropics and midlatitudes. [The mean flow term $(\overline{\sigma v})\overline{\chi}_y$ is comparatively small.] The mixing brings tropical air (low ozone) to the midlatitudes, effecting a negative ozone tendency. A positive tendency is produced in the Tropics as midlatitude air (higher ozone) is mixed equatorward. Both models show about the same amount of horizontal mixing, but the vertical transport by the residual circulation is significantly different. In the vertical direction the mean flow term $(\overline{\sigma Q})\overline{\chi}_\theta$ dominates. The residual circulation advects low-ozone air from lower altitudes in the Tropics to the same degree in both models. But in the midlatitudes the downward transport of ozone-rich air is twice as large in the IS-C-46 model compared with IS-H-46.

5. Discussion

Most transport models used for long-term integrations, like our standard model, are run at resolutions that preclude simulations of finescale features such as laminae. An important modeling issue is whether the accuracy of the horizontal mixing is compromised in models that cannot simulate these features. Our results indicate that the rate of horizontal mixing is similar regardless of whether the model simulates finescale features. The horizontal mixing terms for SP-C-29 and SP-C-73 are almost identical (Fig. 7), yet the latter shows some degree of lamination, albeit weak compared with the sondes. The horizontal mixing terms for IS-C-46, which is an isentropic version of SP-C-29, are comparable to the terms for IS-H-46 (Fig. 8). The latter model produces significant lamination probabilities near the vortex edge but neither SP-C-29 nor IS-C-46 shows any lamination. This suggests that global calculations of constituent transport are not compromised when they are performed at coarse resolutions that preclude simulation of finescale features.

a. Simulation of small-scale features

There are several factors that determine whether a transport model will simulate small-scale features such as laminae. They are 1) resolution, 2) vertical velocities and vertical coordinate used in the transport model, and 3) diffusivity of the transport scheme.

1) RESOLUTION

The resolution of the transport model needs to be fine enough to capture the majority of features allowed by the lamina definition chosen. A frequency distribution of laminar thicknesses for extratropical stations [Figs. 7 and 8 from Reid and Vaughan (1991)] shows that the majority of lamina events have thicknesses greater than 500 m. The aspect ratio between horizontal and vertical scales in the extratropical stratosphere should be about 200:1 (Haynes and Anglade 1997). To resolve a lamina feature of 500 m would require a 250-m vertical grid spacing and a 50-km horizontal grid spacing. Models in this study meet the vertical criteria, but a 50-km horizontal grid spacing (0.5° latitude) is currently not computationally feasible. The highest-resolution model in our study (IS-H-46-HR) has 1° latitude grid spacing and yields lamination rates that approach the observations near the polar vortex edge. A lower-resolution version of this model (IS-H-46) yields lower lamination rates. Differences in lamination rates between these two models attest to the importance of horizontal grid resolution.

2) VERTICAL VELOCITIES

The choice of the vertical coordinate usually determines the vertical velocities used in the model and their magnitude will impact the lamination rates in the model. The sigma-pressure formulation requires the use of continuity-derived winds and the isentropic formulation usually uses the heating rates. A sigma-pressure formulation will always need to include the adiabatic component of the velocity resulting in winds of significantly larger magnitude, compared with the isentropic formulation, which needs only the diabatic component. At issue is whether the larger-magnitude winds will reduce the coherency between the vertical and horizontal features, and inhibit lamina formation. That isentropic models have improved vertical coherency compared with sigma-pressure models is mentioned in Johnson et al. (1993) and Zapotocny et al. (1993). They report that their isentropic model is better able to simulate the transport and precipitation of shallow layers of moisture compared with a sigma model. They attribute the success of the isentropic model to its maintenance of the coherent, large-scale ''conveyor belt'' features in the water vapor distribution.

The diabatic winds used in the isentropic models also tend to be smoother compared with those used in the

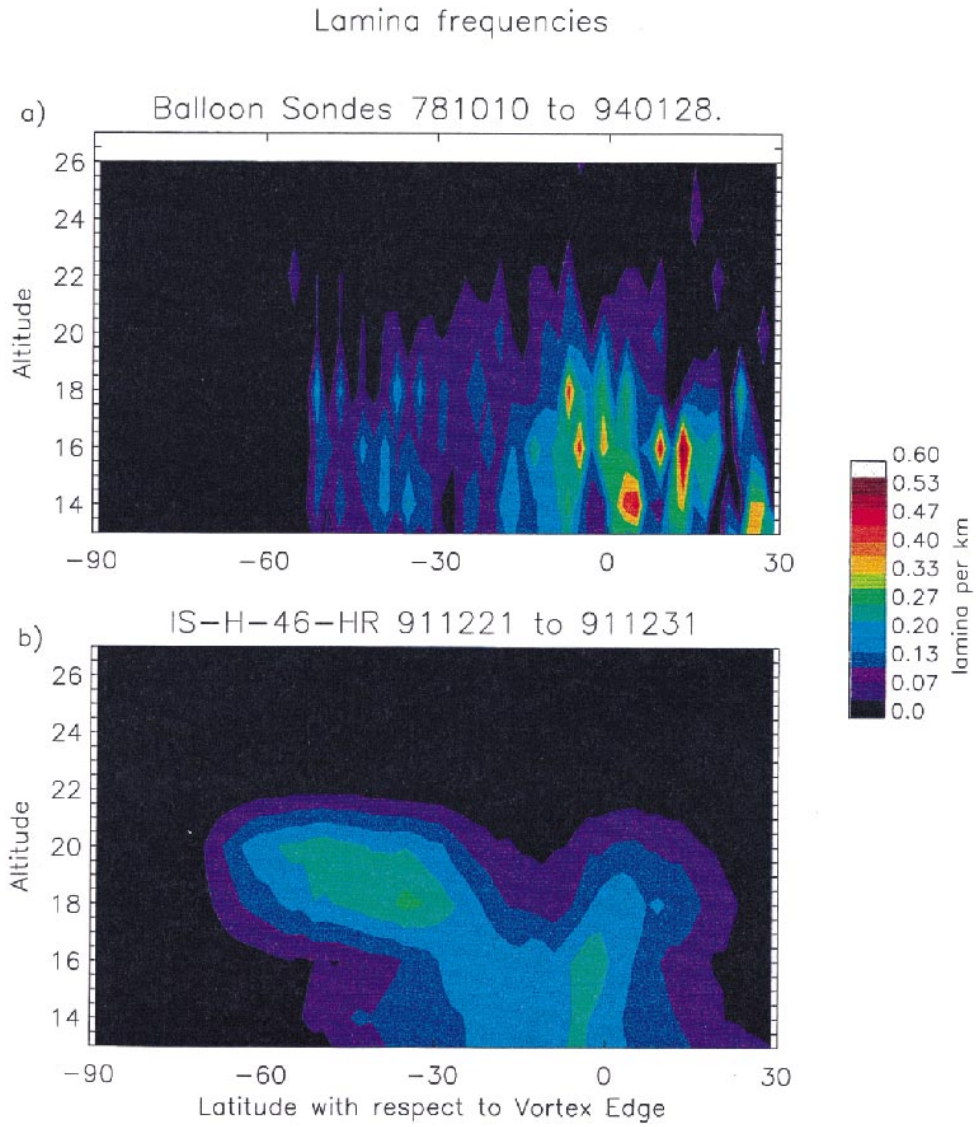

FIG. 5. Lamina frequencies as a function of altitude and the latitudinal distance from the vortex edge: (a) from Dec–Jan climatology of the balloon sondes from 1978 to 1994, vs (b) from 1° latitude by 1.25° longitude isentropic model IS-H-46-HR during the last 10 days of the integration. The units of lamina frequencies are the number of laminar events per km in the vertical.

sigma-pressure formulation. The noise in the assimilated winds might produce excess vertical mixing and destroy any laminar features. Chipperfield et al. (1997) attributes overestimates of the rate of $C1ONO_2$ recovery in the Arctic polar vortex in their isobaric transport model to spurious vertical mixing. Their runs with an isentropic transport model had more realistic rates of $C1ONO_2$ production.

The improved vertical coherency and the smoother vertical winds in the isentropic models explain the higher lamination rates compared with the sigma pressure model SP-C-73. We made every attempt to design the SP-C-73 model to compensate for the stronger and more variable winds that were used. The model accounts for the cross-derivative terms associated with the vertical and horizontal advection and uses a nearly diffusion-free advection scheme. Even with these added features it still yielded lower lamination rates compared with the isentropic models.

3) DIFFUSIVITY OF TRANSPORT SCHEME

We tested whether the level of diffusion in the PPM advection schemes used in our models was sufficiently low to prevent degradation of the lamina features. We advected a hypothetical lamina, in the form of a rectangular wave, back and forth in a one-dimensional model and measured its erosion with time. Grid points were

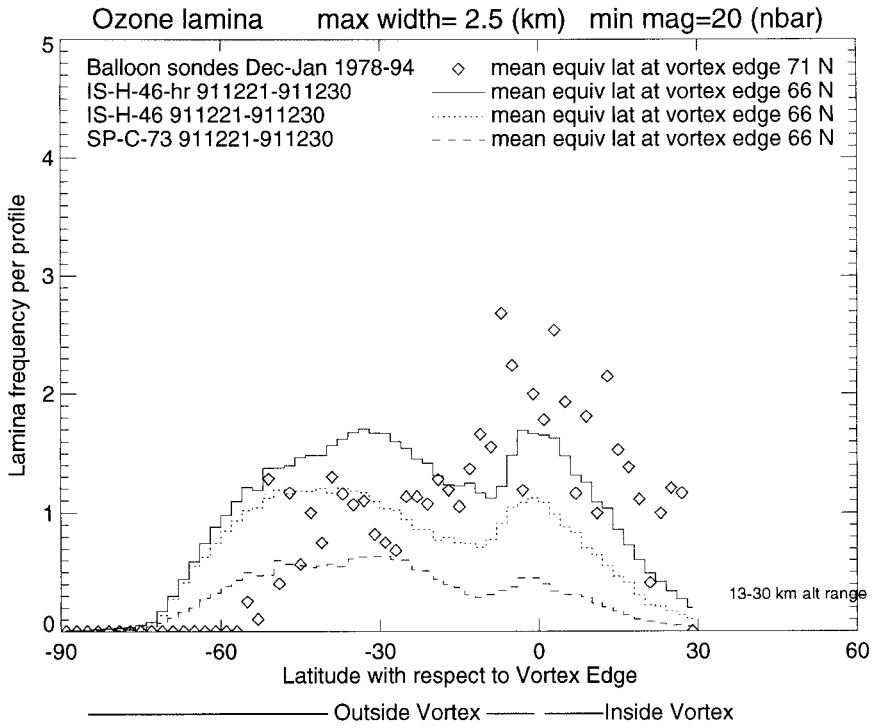

FIG. 6. Model lamination frequencies vs latitudinal distance from the vortex edge between 13 and 30 km. The model frequencies are from the 1° latitude by 1.25° longitude horizontal grid spacing IS-H-46-HR (solid), the 2° latitude by 2.5° longitude grid spacing IS-H-46 isentropic model (dotted), and the SP-C-73 model (dashed) during the last 10 days of the integration. The diamonds are frequencies from a Dec–Jan climatology of the balloon sondes from 1978 to 1994.

spaced every 200 m and the thickness of the lamina varied from 200 m to 2.5 km. The range of winds used to advect the feature included typical values of vertical velocities used in the isentropic and sigma-pressure models. After five days of integration there was negligible degradation from the initial peak for all vertical velocities tested. This indicates that the erosion of simulated laminae from the vertical advection scheme is negligible. It does not address the issues of coherency of horizontal and vertical features.

b. Residual circulation and horizontal mixing

Although it is not necessary to simulate finescale features in a global transport model, we can use results from simulations to assess the accuracy of the horizontal mixing in the 3D transport model. In the vicinity of strong horizontal gradients, wind shear peels off material from one air mass, drawing it into the other. In a horizontal plane this material appears as filaments, but there are actually sheets of material that slope, depending on the vertical shear in the horizontal wind (Newman and Schoeberl 1995; Newman et al. 1996; Orsolini et al., 1997). This shear is induced either by gravity waves (Teitelbaum et al. 1994) or by larger-scale waves (Appenzeller and Holton 1997) that will yield local minima or maxima in an ozone profile. In the atmosphere, filaments lose their integrity when they are irreversibly mixed into the surrounding air. But in the standard transport model, destruction occurs when the filament thickness is less than the grid resolution. The small-scale structure that is observed in the sondes, but not in the sigma-pressure simulations, attests to premature mixing in the model.

Insufficient resolution can explain the difference between the simulated and observed lamination frequencies at the vortex edge. An additional consideration is that gravity waves, which are known to produce lamination in the real atmosphere, are not simulated in the insentropic transport model. In the tropical region there is clearly too much lamination at both horizontal resolutions, suggesting that the model horizontal mixing is excessive there.

The constant addition of temperature and geopotential height observations to the assimilation system maintains realistic latitudinal gradients of EPV. However, maintaining a realistic residual circulation and horizontal mixing is more challenging. Early versions of the NASA/Goddard Data Assimilation System did not have a realistic residual circulation. Although improved methods of data insertion have lead to a much more realistic circulation, there is still room for improvement. The excessive horizontal mixing in the subtropics as suggested by the excessive lamination and by Waugh

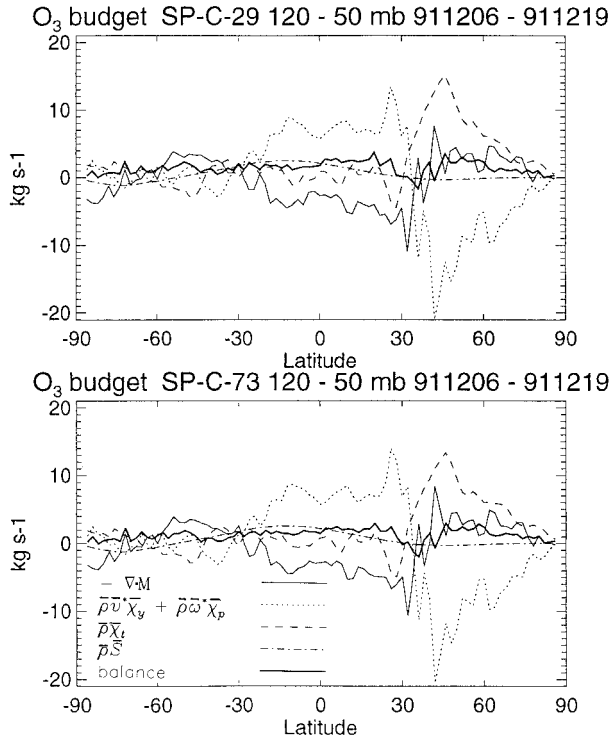

FIG. 7. Budget terms from the advective form of the ozone continuity equation in isentropic coordinates from the isentropic model (a) using heating rates as the vertical velocity IS-H-46 and (b) using continuity-derived vertical velocities IS-C-46. Shown are the meridional (solid) and vertical (dotted) advective terms. Both directions include the mean flow and eddy parts. Also shown is the local zonal mean tendency (broken). The balance of all these terms is due to chemical production and loss (broken dotted).

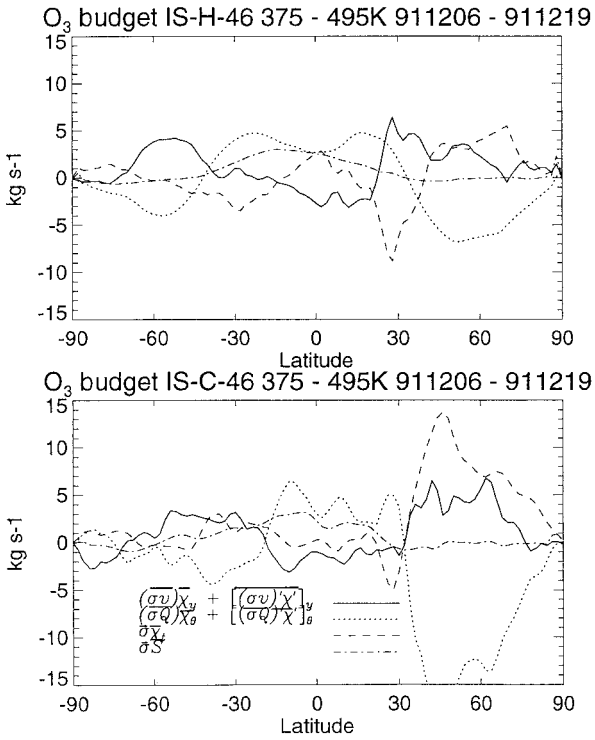

FIG. 8. Budget terms from the advective form of the ozone continuity equation in isentropic coordinates from the isentropic model (a) using heating rates as the vertical velocity IS-H-46 and (b) using continuity-derived vertical velocities IS-C-46. Shown are the meridional (solid) and vertical (dotted) advective terms. Both directions include the mean flow and eddy parts. Also shown is the local zonal mean tendency (broken). The balance of all these terms is due to chemical production and loss (broken dotted).

(1996) may be related to the excessive residual circulation seen in the sigma-pressure simulations. Recall that the sigma-pressure simulations showed a midlatitude buildup of ozone compared with TOMS. It is possible that an excessive residual circulation and excessive horizontal mixing could maintain the correct balance and produce realistic latitudinal gradients of EPV and long-lived tracer.

Results from the isentropic runs using heating rates (IS-H-46) are consistent with this explanation. The residual circulation in the isentropic model, as derived from heating rates, is significantly weaker than the continuity-derived residual circulation but both models have the same amount of horizontal mixing (Fig. 8). Results from IS-H-46 clearly show that the horizontal mixing overwhelms the weaker residual circulation (Fig. 2d).

6. Conclusions

The frequency of lamination appears to be a valuable diagnostic to assess the accuracy of horizontal mixing in wind datasets. Because the Goddard standard transport model is too coarse to resolve laminar events, we developed an isentropic version of the standard Goddard transport model that will produce laminae. Comparison with observations shows that, at least in the vicinity of the polar vortex, the isentropic model lamination frequencies are reasonably accurate. This suggests that the assimilated winds contain the information necessary to produce lamination, even though subscale features are not apparent in a simulation. However, in the subtropics the lamination is excessive compared with the balloon sonde observations and indicates that there is too much horizontal mixing in the isentropic transport model. Budget calculations show that the standard transport model and the isentropic model have similar amounts of horizontal mixing, suggesting that the excessive mixing also applies to the standard sigma-pressure model. Increasing the horizontal resolution of the standard transport model has almost no effect on the ozone spatial distribution. This suggests that the excessive mixing is not from too coarse a grid resolution but instead is inherent in the assimilated winds. Finally, the similar horizontal mixing terms in the isentropic and standard model indicate that the resolution of the standard model is sufficient for simulating the global distribution of a constituent. Global calculations of constituent transport are

not compromised when performed at resolutions of our standard model that are too coarse to simulate finescale features.

Acknowledgments. We thank Paul Newman and Larry Coy for constructive comments on this manuscript. This work was supported by NASA's Atmospheric Effects of Stratospheric Aircraft Program and by the NASA Atmospheric Chemistry Modeling and Analysis Program. Computer support was provided by the Earth Observing System Program.

REFERENCES

Allen, D. J., A. R. Douglass, R. B. Rood, and P. D. Guthrie, 1991: Application of a monotonic upstream transport scheme to three-dimensional constituent transport calculations. *Mon. Wea. Rev.*, **119,** 2456–2464.

Andrews, D. G., J. R. Holton, and C. B. Leovy, 1987: *Middle Atmosphere Dynamics.* Academic Press, 489 pp.

Appenzeller, C., and J. R. Holton, 1997: Tracer lamination in the stratosphere: A global climatology. *J. Geophys. Res.,* **102,** 13 555–13 569.

Chipperfield, M. P., 1999: Multiannual simulations with a three-dimensional chemical transport model. *J. Geophys. Res.,* **104,** 1781–1805.

——, E. R. Lutman, J. A. Kettleborough, J. A. Pyle, and A. E. Roche, 1997: Model studies of chlorine deactivation and formation of $ClONO_2$ collar in the Arctic polar vortex. *J. Geophys. Res.,* **102,** 1467–1478.

Douglass, A. R., C. H. Jackman, and R. S. Stolarski, 1989: Comparison of model results transporting the odd nitrogen family with results transporting separate odd nitrogen species. *J. Geophys. Res.,* **94,** 9862–9872.

——, C. J. Weaver, R. B. Rood, and L. Coy, 1996: A three-dimensional simulation of the ozone annual cycle using winds from a data assimilation system. *J. Geophys. Res.,* **101,** 1463–1474.

Haynes, P., and J. Anglade, 1997: The vertical-scale cascade in atmospheric tracers due to large-scale differential advection. *J. Atmos. Sci.,* **54,** 1121–1136.

Jackman, C. H., E. L. Fleming, S. Chandra, D. B. Considine, and J. E. Rosenfield, 1996: Past, present, and future modeled ozone trends with comparisons to observed trends. *J. Geophys. Res.,* **101,** 28 753–28 767.

Johnson, D. R., T. H. Zapotocny, F. M. Reames, B. J. Wolf, and R. B. Pierce, 1993: A comparison of simulated precipitation by hybrid isentropic-sigma and sigma models. *Mon. Wea. Rev.*, **121,** 2088–2114.

Lary, D. J., M. P. Chipperfield, W. A. Norton, J. A. Pyle, and L. P. Riishojgaard, 1995: Three-dimensional tracer initialization and general diagnostics using equivalent PV latitude-potential-temperature coordinates. *Quart J. Roy. Meteor. Soc.,* **121,** 187–210.

Lin, S. J., and R. B. Rood, 1996: Multidimensional flux-form semi-Lagrangian transport schemes. *Mon. Wea. Rev.,* **124,** 2046–2070.

Mahlman, J. D., 1985: Mechanistic interpretation of stratospheric tracer transport. *Advances in Geophysics,* Vol. 28, Academic Press, 301–323.

Nash, E. R., P. A. Newman, J. E. Rosenfield, and M. R. Schoeberl, 1996: An objective determination of the polar vortex using Ertel's potential vorticity. *J. Geophys. Res.,* **101,** 9471–9478.

Newman, P. A., and M. R. Schoeberl, 1995: A reinterpretation of the data from the NASA Stratosphere–Troposphere Exchange Project. *Geophys. Res. Lett.,* **22,** 2501–2504.

——, and Coauthors, 1996: Measurements of polar vortex air in the midlatitudes. *J. Geophys. Res.,* **101,** 12 879–12 891.

Orsolini, Y. J., P. Simon, and D. Cariolle, 1995: Filamentation and layering of an idealized tracer by observed winds in the lower stratosphere. *J. Geophys. Res.,* **100,** 839–842.

——, G. Hansen, U.-P. Hoppe, G. L. Manney, and K. H. Fricke, 1997: Dynamical modelling of wintertime lidar observations in the Arctic: Ozone laminae, and ozone depletion. *Quart. J. Roy. Meteor. Soc.,* **123,** 785–800.

Reid, S. J., and G. Vaughan, 1991: Lamination in ozone profiles in the lower stratosphere. *Quart. J. Roy. Meteor. Soc.,* **117,** 825–844.

——, ——, and E. Kyro, 1993: Occurrence of ozone laminae near the boundary of the stratospheric polar vortex. *J. Geophys. Res.,* **98,** 8883–8890.

Riishojgaard, L. P., and E. Kallen, 1997: On the correlation between ozone and potential vorticity for large scale Rossby waves. *J. Geophys. Res.,* **102,** 8793–8804.

Rood, R. B., and Coauthors, 1991: Three-dimensional simulations of wintertime ozone variability in the lower stratosphere. *J. Geophys. Res.,* **96,** 5055–5071.

Schoeberl, M. R., and Coauthors, 1989: Reconstruction of the constituent distribution and trends in the Antarctic polar vortex from ER-2 flight observations. *J. Geophys. Res.,* **94,** 16 815–16 845.

Schubert, S. R., R. B. Rood, and J. Pfaendtner, 1993: An assimilated dataset for earth science applications. *Bull. Amer. Meteor. Soc.,* **74,** 2331–2342.

Takacs, L. L., and M. J. Suarez, 1995: Documentation of the ARIES/GEOS Dynamical Core Version 2. NASA Tech. Memo. 104606, 201 pp. [Available from NASA Center for AeroSpace Information, 800 Elkridge Landing, Linthicum Heights, MD 21090-2934.]

Teitelbaum, H., J. Ovarlez, H. Kelder, and F. Lott, 1994: Some observations of gravity-wave-induced structure in ozone and water vapour during EASOE. *Geophys. Res. Lett.,* **21,** 1483–1486.

Waugh, D. W., 1996: Seasonal variation of isentropic transport out of the tropical stratosphere. *J. Geophys. Res.,* **101,** 4007–4023.

Weaver, C. J., A. R. Douglass, and R. B. Rood, 1993: Thermodynamic balance of three-dimensional stratospheric winds derived from a data assimilation procedure. *J. Atmos. Sci.,* **50,** 2987–2993.

Zalesak, S. T., 1979: Fully multidimensional flux-corrected transport algorithms for fluid. *J. Comput. Phys.,* **31,** 335–362.

Zapotocny, T. H., D. R. Johnson, and F. M. Reames, 1993: A comparison of regional isentropic-sigma and sigma model simulations of the January 1979 Chicago blizzard. *Mon. Wea. Rev.,* **121,** 2115–2135.